Analysis of Spectrum Access Techniques in Unlicensed Frequency Bands

Rita Bandeira
rita.bandeira@ist.utl.pt

Instituto Superior Técnico, Lisboa, Portugal

May 2017

Abstract

While Short Range Devices (SRDs) already have a relevant presence in networks today, ranging from remote control to wireless sensors, it is expected that in the next decade their number will increase considerably. SRDs operate in unlicensed spectrum, and though there are some rules to control the sharing of radio resources, there is no limit to the geographical density of devices. Therefore, an efficiency in radio resource utilization is of paramount importance to guarantee the expected performance, even in high contention situations. It is also necessary to guarantee that the growing number of SRDs operating in the adjacent band of Long Term Evolution (LTE) do not degrade its performance, and vice-versa. In this work, a simulator was developed in order to analyze two mechanisms for channel access – Duty Cycle (DC) and Carrier Sense Multiple Access (CSMA) – in a building automation application scenario (e.g., a room temperature control system) and considering multiple SRD densities. Both these channel access schemes were evaluated independently and in a coexistence scenario. Results have shown that CSMA clearly outperforms DC, yielding lower Packet Loss Rates (PLR). Moreover, CSMA is proven to successfully operate in the presence of dozens of DC sensors, while the contrary is not true. Finally, the results for LTE and SRD coexistence show that LTE User Equipment emissions can cause packet collisions in SRDs for low SRD transmission powers. On the other hand, the impact of SRD emissions on LTE UEs is insignificant.
Keywords: Short Range Devices, Duty Cycle, Carrier Sense Multiple Access, Listen Before Talk, Unlicensed Frequency Bands

1 Introduction

Short Range Devices (SRD) are present in a vast variety of applications, from the most simple ones, like remote controls in car keys, to the most complex, such as industrial automation systems, covering a wide range of requirements. A key characteristic they share, in general, is free access to the licence-exempt frequency bands. This implies that there is competition for radio resources from different devices or even applications.

The channel access mechanisms play a critical role in the efficiency of channel utilization. SRDs can access the channel synchronously or asynchronously. Synchronous mechanisms require some sort of centralized control of the devices, increasing system complexity and cost, and are generally used for critical applications in terms of quality of service. The vast majority of SRDs, however, use asynchronous channel access schemes, which is a more suitable solution for low-cost and simple applications.

Asynchronous channel access schemes are specially relevant in the SRD landscape mainly due the simplicity of the devices (e.g., sensors, remote controls). For their relevance, two widely-used asynchronous channel access schemes are studied in this work. Not only their performance, but also their coexistence is analysed.

1.1 Objectives

The objective of this work is to analyse two channel access schemes: DC and nonpersistent-CSMA. For that purpose, a simulator was developed in C language, implementing a simulated sensor network for a building automation scenario. The two channel access schemes are studied in terms of their individual performance, as well as their coexistence. Finally, the impact of LTE's frequency spill in the SRD network is analysed, and vice-versa.

1.2 Structure

This article is organized as follows: section 1 introduces and contextualizes the work; section 2 briefly describes the channel access schemes in study; section 3 describes the simulator and model implementation; section 4 presents the simulation results and

main conclusions.

2 Channel Access Schemes

The way SRDs communicate directly impacts the overall performance. Mainly, channel access techniques have two distinct approaches: **contention** and **schedule-based**. Simply put, in contention-based techniques, nodes contend for the channel in an independent and random way, which may result in a packet collision. In schedule-based (or collision-free) approaches there is some control unit that assigns different time/frequency slots to each SRD, avoiding collisions altogether within the system (note that it is still vulnerable to external interference). Both algorithms in study are contention-based.

2.1 DC

Duty cycle (DC) is simplest form of random channel access. Its name derives from the fact that devices are only active for a very short period of time (usually ms), periodically. During the remaining time, they are in sleep mode spending practically no energy. The DC value represents the percentage of time the device is transmitting within a cycle:

$$DC = \frac{T_p}{T_{cycle}}. \tag{1}$$

where T_p is the packet duration and $T - cycle$ is the packet period duration (at the application layer).

The Packet Loss Rate (PLR) of a DC system, considering all nodes in the network can cause collisions on one-another, can be computed as [2]:

$$PLR = 2DC^{N-1}. \tag{2}$$

2.2 CSMA

Carrier Sense Multiple Access (CSMA) protocols are based on a Listen Before Talk (LBT) behaviour: instead of blindly transmitting, the channel is first sensed and if activity is detected, the node refrains from transmitting immediately. From the existing versions of the CSMA algorithm, the one used in this work is the nonpersistent-CSMA (np-CSMA), which is characterized by the following: if a device senses the channel is busy, it postpones a new sensing to a random time in the future.

3 Simulation of Channel Access Schemes

3.1 Simulation Scenario

The simulation scenario emulates a sensor network in a close-to-real indoor environment. It considers path loss due to signal propagation and noise. Due to the typical short distances between devices in sensor networks (up to some dozens of meters) however, the propagation delay is assumed to be zero. More specifically, this scenario models a building automation system in an open space office environment. In this type of network, sensors and actuators

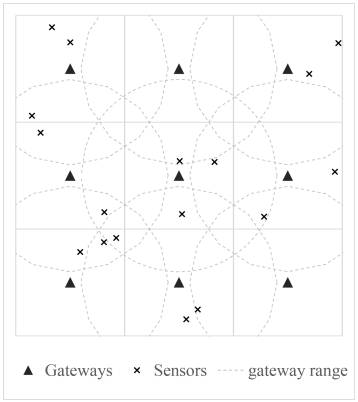

Figure 1: Network node placement example.

are used to monitor and operate, for instance, electrical and air conditioning systems, electric shutters and different types of alarms (e.g., fire/smoke and intrusion) [4]. When initializing the simulation, network nodes are randomly placed in the environment, while gateways have fixed positions as illustrated in Figure 1 (which emulates, for instance, a scenario where low-range gateways are incorporated into lamps placed on the ceiling). A star (or one-hop) topology was chosen, due to its simplicity and independence of routing algorithms (which are not within the scope of this work) – all sensors are directly connected to a gateway, which is power plugged, and therefore constantly listening to channel activity, while sensors compete for access to the channel by using a given channel access scheme. Sensors communicate with the gateway they are closer to.

A message can only be correctly received and demodulated if the signal to interference plus noise ratio (SINR) at the receiver is above a given threshold:

$$sinr > sinr_{min}. \tag{3}$$

The SINR is defined, in linear units, by the ratio between the useful signal power, p_r, and the sum of the interfering signal powers, $i_{r,k}$, and the noise power at the receiver, n:

$$sinr = \frac{p_r}{\sum_k i_{r,k} + n}. \tag{4}$$

By manipulating inequality (3) and equation (4), one can obtain an expression for the maximum value of the total interfering power that allows for a correct reception of the signal:

$$\sum_k i_{r,k} < \frac{p_r}{sinr_{min}} - n. \tag{5}$$

Since, for a given sensor, we consider p_r to be constant and $sinr_{min}$ and n are characteristic of

the receiver (and hence also constant), to evaluate if a packet collision occurred, one needs simply to evaluate at any given time if the current interference from all active transmitters is greater than this value – which will be denoted as interference limit, i_{lim}:

$$i_{lim} = \frac{p_r}{sinr_{min}} - n. \quad (6)$$

The signal power received by node i when node j was transmitting is calculated by dividing the power emitted by transmitter i, $p_{t,i}$ by the path loss between the nodes, pl_{ij} (note that this computation is valid for both useful and interfering signals):

$$p_{r,j} = \frac{p_{t,i}}{pl_{ij}}. \quad (7)$$

The path loss model for indoor environments is defined in ITU Recommendation [3], which estimates the total path loss PL, in dB, as:

$$PL_{dB} = 20\, log(f_{[MHz]}) + 10\, a\, log(d_{[m]}) + L_f(s) - 28, \quad (8)$$

where f is the carrier frequency in MHz, a is the path loss exponent, d is the distance between the transmitter and the receiver in meters and $L_f(s)$ is the additional loss factor caused by the penetration of s floors or walls, in dB. For the present simulated office environment, theses standard values apply [3]: loss exponent of $a = 3.3$. Since a single floor is considered in the simulation, $L_f = 0$.

One of the factors to consider when calculating a node's range is the receiver's sensitivity, P_{det}, which is the minimum signal power it can detect. Assuming a node i transmitting with power $P_{t,i}$ (dBW), at a distance d from the receiver j, the received power $P_{r,j}$ (dBW) is calculated from (7). In logarithmic units, equation (7) translates to

$$P_{r,j} = P_{t,i} - PL_{ij}. \quad (9)$$

To compute the nodes' range, r, the maximum path loss between nodes, PL_{max}, is calculated for a received power that equals the sensitivity, $P_r = P_{det}$, resulting in:

$$PL_{max} = P_t - P_{det}. \quad (10)$$

By solving equations (8) and (10) in d, the range can be obtained:

$$r = f^{-\frac{2}{a}}\ 10^{\frac{P_t + 28 - L_f - P_{det}}{10\ a}}. \quad (11)$$

Finally, noise power in the receiver is computed as the product of the input thermal noise power n_0 and the device noise factor n_f:

$$n = n_0\ n_f. \quad (12)$$

In its turn, the thermal noise power, n_0, is dependent on the temperature and receiver's bandwidth. By multiplying the receiver's bandwidth B and the noise spectral density, $k\ T$, where k is the Boltzmann's constant and T the receiver's absolute temperature, the thermal noise power can be obtained:

$$n_0 = k\ T\ B. \quad (13)$$

Throughout the work, an ambient temperature of $T = 290\ K$, corresponding to normal temperature and pressure conditions (NPT), was assumed. A typical noise figure value for this type of devices of $N_f = 3$ dB was considered, corresponding to a noise factor of $n_f = 10^{N_f/10} \approx 2$ [5]. Finally, a bandwidth of $B = 200$ kHz, which is typical for SRD applications in this frequency band was used [2].

3.2 Simulator Implementation

The simulator was developed in the C programming language using an event-based approach: modelled actions, such as transmitting a data packet or probing channel activity, are represented by events that mark their start and end moments in time. Events are stored in a list, ordered by their occurrence time. Throughout the simulation, events are "pulled" from the list and, depending on the type of event, the correspondent actions are taken.

Apart from the event list, all other program's variables were grouped into four categories: **input parameters**, **status variables**, **counters** and **outputs**. Input parameters variables store all the information that was extracted from the input file during initialization; status variables have information regarding the current status of each node (including, for instance, the current received interference power and flags to indicate if the sensor is listening); counters store the current number of certain occurrences in each node (such as lost packets or received ACKs); finally, outputs store the results of the simulation and are computed using the counters' values (e.g. PLR equals one minus the number of successfully delivered packets divided by the number of packets from the application layer to be transmitted). Each category was implemented as a `struct` variable, in a "container-like" fashion, including all correspondent variables within the structure. By encapsulating variables in structures, extending the program's functionalities becomes easier, since variables can be added inside each structure without the need for changes in the program's `main` function.

Since the size of the event list varies constantly, a linked list structure is the most suitable choice in this case. For the majority of other variables, when one value per sensor node is needed, one and two-dimensional arrays were used.

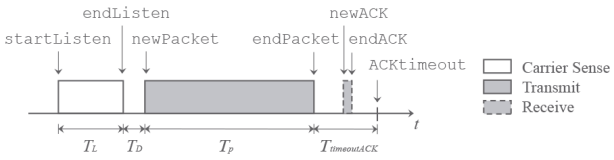

Figure 2: Simulated events and correspondent physical phenomena.

The program starts with reading an input file with the simulation parameters. Since most of the results are analysed as a function of the number of sensors in the network, N_S, the option of running the simulator for several values of N_S was taken. All the N_S values to be simulated are stored in an array, `nList`, and the simulations are run for each of them. The program finishes when the end of the array is reached. For each N_S, `S` simulations are run (the counter `nsimulated` registers how many simulations have been run to the moment) and for each simulation, the memory for all the variables is allocated upon the simulation initialization process and freed in the end. After the initialization, the simulated time `Tsim` is reset. Every time an event is pulled from the event list, the simulation time is updated to the time of occurence of the event, `Te`. Afterwards, the function correspondent to the type of event is called. The mapping of the implemented events and their correspondent physical phenomena is depicted in Figure 2. It can be observed that each event corresponds to either a start or end of some action. The functions called for each event have the specific algorithms for the channel access scheme in question. The simulation ends when a predefined time limit, `Tmax`, is exceeded.

4 Results

From the frequencies that the MICA2 MpR400CB [6] sensor can work with, the 868 MHz frequency was chosen for the following reasons: 1) it resides in the 863-870 MHz unlicensed frequency band for SRDs; 2) within this band, the 868-868.6 MHz subband is the one closest to the LTE band (below 863 MHz) that hosts the type of applications within the scope of this work. A DC of 1% was used in the CSMA simulations, while a more conservative DC value of 0.1% was used for the DC system. In terms of the packet size, the limit value of 300 bits for a small packet was considered. The MICA2 sensor takes approximately 15.6 ms to transmit 300 bits, therefore, the packet size, for the sake of simplicity, was assumed to be $T_p = 15$ ms. Finally, the maximum admissible PLR value (at the MAC layer) was determined to be 1%, as referred in [4] and considering the applications in place are of a less critical nature – excluding, for instance, alarms, which have a higher reliability requirement. Apart from the DC value, all other parameters are shared by the DC and CSMA systems.

The default building dimensions were determined so as to guarantee full coverage for the minimum transmission power, considering all the gateways are placed in a grid. In all simulations, 16 gateways were used, resulting in a square building with 152 m × 152 m – these values were chosen so as to have a fairly large area, while still making sense in a real-life scenario.

The Monte Carlo method [7] was applied in order to increase the accuracy of the results. The results are presented with a 95% confidence interval.

4.1 DC

In order to determine the effect of the transmission power, P_t, on the system performance, a minimum interference distance, d_{Imin}, between the interferer and the victim (a gateway or a sensor) can be computed, so that if the interferer is at a distance greater that d_{Imin}, the interference would not be enough to cause a collision. From (6) and (7), d_{Imin} can be computed for the limit case, with the following considerations: 1) the received interfering power, P_{rI}, equals the interference limit $P_{rI} = I_{lim}$; 2) the sensor is at the gateway's range limit: $P_r = P_{det}$; 3) the noise power, n, is negligible[1] compared to $p_r/sinr_{min}$, resulting in $I_{lim} \approx P_r - SINR_{min}$. The minimum interference distance can then be obtained as follows:

$$d_{Imin} = d\ 10^{\frac{SINR_{min}}{10a}}. \qquad (14)$$

where d is the distance between the sensor and the gateway. It can be concluded that the minimum interference distance does not depend on the transmitted power, but on the distance between the gateway-sensor pair: the closer the sensor is to the gateway, the smaller d_{Imin}.

The simulation results for a DC system with DC = 0.1% as a function of the transmitted power are shown in Figure 3. The results show that the PLR does not depend on the transmitted power, as was demonstrated in Equation (14). In the same Figure, it can be seen that the PLR is significantly lower than the theoretical value. This can be explained by the sensors' proximity to gateways: by adding more gateways in the same building, sensors can be closer to a gateway, thus increasing the minimum interfering distance – and becoming "immune" to interference from sensors within that distance; the theoretical value of DC PLR corresponds

[1] For the maximum sensor-gateway distance of $d = 27$ m and the minimum transmitted power, $P_t = -20$ dBm, the noise power results in $n \approx 1.6 \times 10^{-16}$ W; for the same distance and power values, $p_r/sinrmin \approx 1.6 \times 10^{-15}$ W. Since the noise power is ten times smaller than $p_r/sinr_{min}$, it is considered negligible.

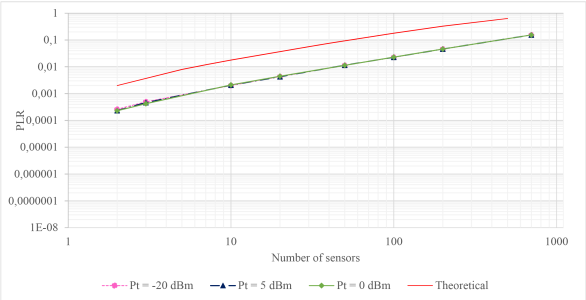

Figure 3: PLR of a DC system with $DC = 0.1\%$ as a function of the transmitted power.

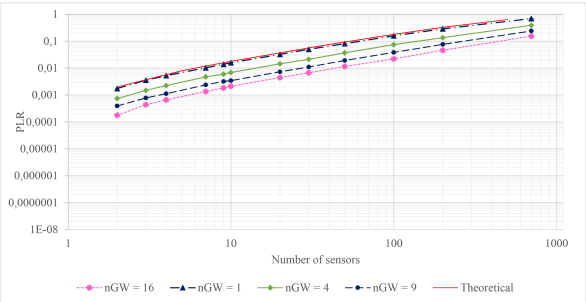

Figure 4: PLR of a DC system with $DC = 0.1\%$ as a function of the number of gateways.

to the case where all sensors can interfere with one-another (which is similar to a scenario with only one gateway). This result can be observed in Figure 4: as the number of gateways inside the building increases, the PLR decreases, since the distance between sensors and gateways is smaller. In the limit case of only one gateway, the PLR is equal to the theoretical one, from Equation (2). This result shows that a number of 16 gateways, while being adequate for a real-life implementation of a sensor network in this scenario, can significantly reduce the PLR of the DC system. The same is true for CSMA, although the study of the impact of the number of gateways on the CSMA PLR is out of the scope of the work.

4.2 CSMA

The PLR results for the CSMA system are in Figure 5. As can be observed, the PLR linearly increases with the transmitted power, with the exception of $P_t = -20$ dBm. This can be explained by the hidden node effect. A sensor can detect transmitters that are within its range, r, and can suffer collisions from transmitters that are within its minimum interfering distance, d_{Imin}. For the case of $P_t = -20$ dBm, the range is approximately $r = 27.0$ m, while $d_{Imin} = 52.6$ m for the worst case scenario (the sensor is as far as possible from the gateway). The range is significantly smaller

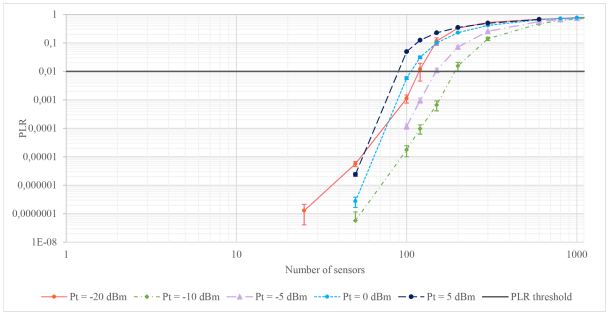

Figure 5: PLR of a CSMA system as a function of the transmitted power.

than the interfering distance, creating the conditions for false negatives to occur – there are potential interferers within collision range that the sensor cannot detect. This effect can be seen in Figure 6, where the collision rate for this case is much higher. For the case of $P_t = -10$ dBm, however, the distances become closer in value: $r = 54.2$ m (and $d_{Imin} = 52.6$ m as previously mentioned, since it does not depend on the transmitted power). In this case, most nodes would be able to successfully detect all the interferers within collision range. If we consider higher values of P_t, on the other hand, false positives become a problem. The range is much larger than the minimum interference distance (e.g. for $P_t = 0$ dBm, $r = 109.0$ m), which means that sensors can detect far-away transmitters that they would not collide with, thus wrongly refraining from transmitting. This can be observed in Figure 7, where the transmission rate is shown as a function of P_t. The transmission rate is defined as the average number of transmissions (successful or not) per cycle. The higher the power, the lower the transmission rate, which indicates the presence of false positives. Furthermore, the effect of the false negatives for $P_t = -20\ dBm$ is also clear, since collisions increase the number of retransmissions. In conclusion, the transmitted power that provides the best PLR results is the one that corresponds to the case where the minimum interference distance, d_{min}, approaches the range, r.

For the rest of the simulations in the present section, the transmitting power of $P_t = -10\ dBm$ is used, since it represents the case with the best PLR, from the ones that were simulated.

4.3 DC and CSMA Coexistence

In Figure 8, the PLR of the CSMA system can be observed as a function of the number of interfering DC sensors, N_{DC}. It can be concluded that the presence of the DC system does not significantly impair the CSMA PLR. Furthermore, the maximum number of CSMA sensors in the network, corresponding to the maximum admitted PLR (1%),

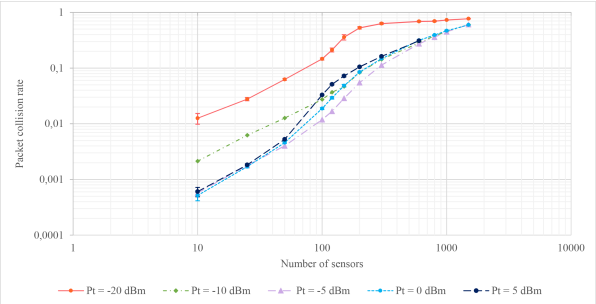

Figure 6: Collision loss rate of a CSMA system as a function of the transmitted power.

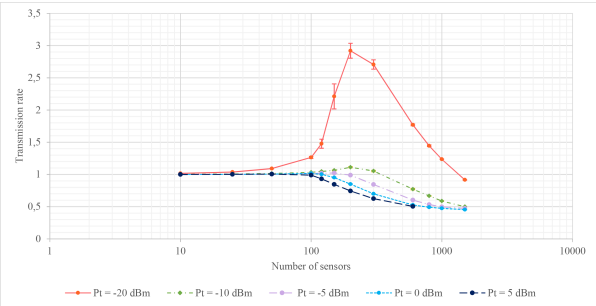

Figure 7: Transmission rate of a CSMA system as a function of the transmitted power.

almost does not vary, as can be seen in Figure 9. Although the PLR is not significantly higher, the effect of the interference of the DC can be observed in Figures 10 and 11: both the collision rates and the ACK loss rate, respectively, are significantly affected by the interference of the DC system, for lower values of N_{CSMA}. It can, therefore, be concluded that the presence of a DC system, with $DC = 0.1\%$, does not significantly impair the CSMA PLR, although it causes an increase in the number of retransmissions due to collisions and loss of ACK packets, which proportionally increases the energy spent by the sensors. In the case of systems that are highly energy-constrained, this effect could mean that the two systems cannot coexist.

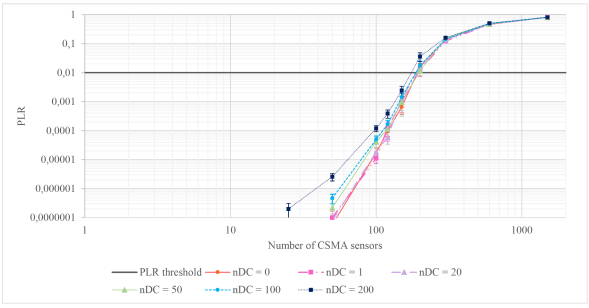

Figure 8: PLR of the CSMA system as a function of the number of CSMA and DC sensors.

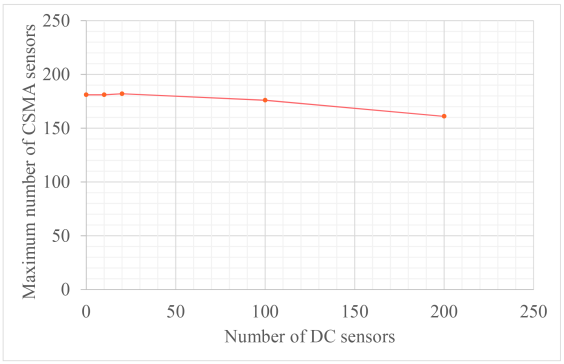

Figure 9: Maximum number of CSMA sensors (for a maximum PLR of 1%) as a function of the number of DC sensors.

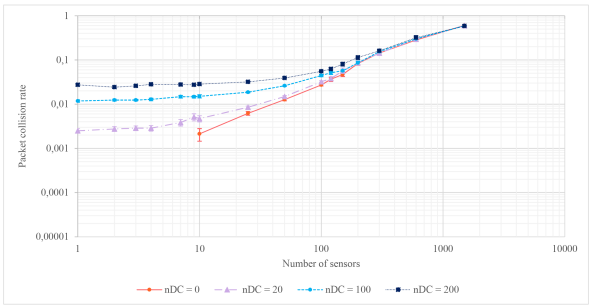

Figure 10: Collision loss rate of the CSMA system as a function of the number of CSMA and DC sensors.

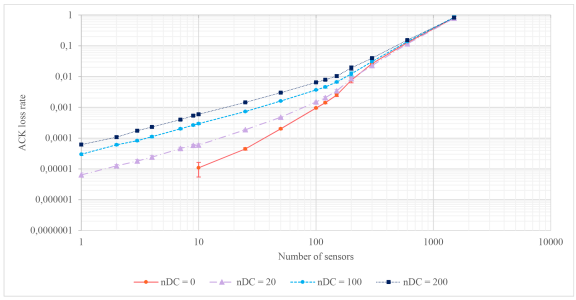

Figure 11: ACK loss rate of the CSMA system as a function of the number of CSMA and DC sensors.

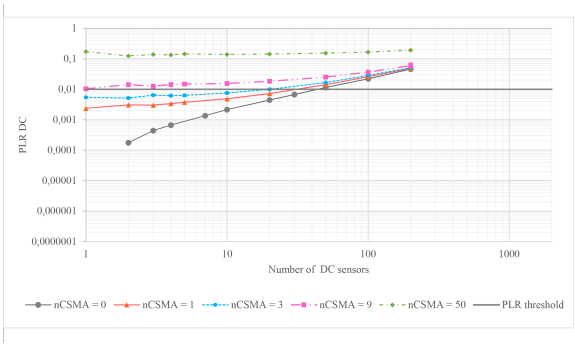

Figure 12: PLR of the DC system as a function of the number of CSMA and DC sensors.

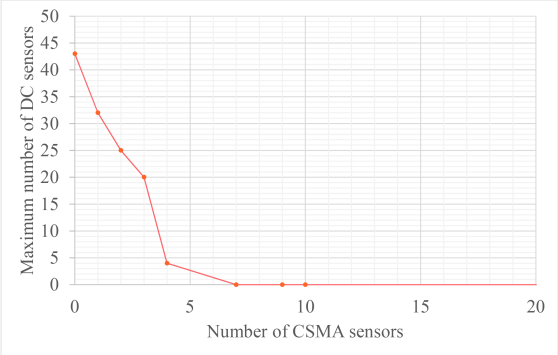

Figure 13: Maximum number of DC sensors (for a maximum PLR of 1%) as a function of the number of CSMA sensors.

On the other hand, the DC system suffers considerable degradation due to the presence of the CSMA system. In Figure 12, the PLR of the DC system increases significantly with each added CSMA sensor. This can be explained by the fact that the CSMA system has a *DC* value that is ten times higher, which means that, in practice, adding one CSMA sensor creates up to as much traffic as 10 DC sensors, and thus having a considerate impact. In Figure 13, the maximum number of DC sensors (for a maximum PLR of 1%) as a function of CSMA sensors is represented. As it can be observed, the maximum number of DC sensors reaches zero for only 7 CSMA sensors, which means that the DC system cannot coexist with a CSMA system with 7 or more sensors. In practice – and since CSMA networks can work with far more sensors than this – it can be concluded that DC systems cannot coexist with CSMA systems.

Finally, the conclusion to be taken from the present analysis is that a CSMA system can mitigate the interference caused by a DC system by increasing the number of retransmissions. A DC system, on the other hand, suffers such a degradation from the CSMA interference that it makes the coexistence not feasible.

4.4 SRD and LTE Coexistence

As proven by (14), the closer the sensor and gateway are, the closer that an interferer can be without causing collisions – more specifically, this equation determines the minimum distance between the interferer and the victim (sensor/gateway) for collision-free communication as a function of the sensor-gateway distance.

This analysis, on the other hand, was carried out by determining the maximum distance between the sensor and the gateway, d_{max}, as a function of the distance between the UE and the victim (sensor/gateway), d_{UE}, in order for the UE not to cause collisions (by itself) in the information received at this node. This means that, for a UE interferer with a known position, a circle of radius d_{max} can be drawn around each gateway – and every sensor within this area (with $d < d_{max}$) can send its information to the gateway without collisions directly caused by the UE; if, on the other hand, the sensor is outside the area (with $d < d_{max}$), the corresponding gateway is vulnerable to the effects of the UE interference. This circular area around the gateways is called an inclusion zone, while the area outside the circle is the exclusion zone.

Similarly, d_{max} and the correspondent inclusion zone can be determined for sensors. In this case, the gateway needs to be inside the sensor's inclusion zone in order for the ACKs to be correctly received at the sensor without being affected by the UE's interference.

In short, an inclusion area can be defined around either the gateway or the sensor. The sensor-gateway pair can only be completely immune to the UE's interference if they are both inside one another's inclusion areas, meaning that neither the sensor packets or the ACKs suffer from the UE's interference. The maximum sensor-gateway distance can indicate, in general terms, if an SRD network could coexist with LTE UEs: if d_{max} is too small, it means that coexistence is not feasible, and vice-versa.

In this analysis, only the UE interference at the gateways is considered, since it is this situation that directly affects the SRD system's PLR (UEs could also cause collision on ACKs received by the sensors, although that would only increase the energy spent for additional retransmissions, since the information was effectively received at the gateway – it was only the ACK that was lost).

Similarly to (14) (and also considering that $I_{lim} \approx P_r - SINR_{min}$), the d_{max} expression can be computed from (6) and (9), resulting in:

$$d_{max} = d_{UE}\ 10^{\frac{P_t - P_{tUE} - SINR_{min}}{10a}}, \qquad (15)$$

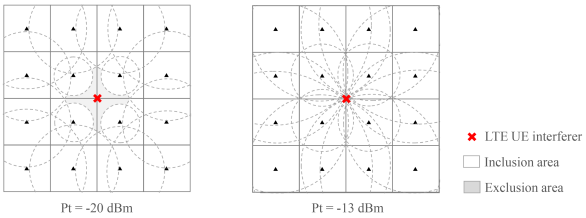

Figure 14: Inclusion area around gateways for one UE interferer.

where $P_{tUE} = -20$ dBm is the power spill of the UE into the SRD frequency channel in use (as computed from LTE's maximum transmitted frequency and emmisison mask, from [1]) and d_{UE} is the distance between the UE and the gateway.

Let us consider the UE is inside the building and at its center. The exclusion zone for the gateways within the building is depicted in Figure 14, for $P_t = -20$ dBm. As it can be observed, there is an exclusion area of significant size, meaning that a UE could hardly work inside the building without impairing the CSMA system. Increasing the SRD system's power mitigates this problem. By increasing P_t, the inclusion area expands – and it can expand so as to include the UE itself, which means in practice that the UE power, P_{tUE}, is not enough to cause interference on the gateway-sensor pair. Having said this, the limit for the inclusion of the UE in the inclusion area corresponds to $d_UE = d_{max}$, which, from (15), results in $P_t = -13$ dBm. This means that for a transmitted power above -13 dBm, the UE cannot cause cause collisions on the SRD system. Since this power value is possible for SRDs, it can be concluded that SRDs can coexist with at least one LTE UE.

Finally, when considering the possible interference of SRDs on LTE, it can be easily concluded that the impact would be insignificant: considering, similarly to LTE's case, that the frequency spill from SRDs into the UE frequency band is around -30 dB below the transmitted power, a maximum interfering power density of -18 dBm/MHz would be present in the UE upper channel. This value is not significant when compared to the UE's maximum power density (23 dBm/MHz).

Conclusions

The results show CSMA clearly outperforms DC in terms of PLR. Moreover, the PLR of the CSMA system is influenced by the transmitted power, due to the hidden node effect: a low transmission power means a smaller detection range, and therefore the sensor's transmissions suffer collisions from other sensors that it could not detect (i.e. a false negative occurs); on the other hand, a high transmission power results in a large detection range, which in turn means that the sensor repeatedly detects on-going transmissions and refrains from transmitting, when in fact they would not have caused a collision (a false positive takes place). Interferers need to be at a minimum distance from other receivers to cause collisions, and the best PLR-performing transmission power is the one that results in a detection range that is close in value to this minimum distance for collision; in these conditions, the sensor can detect all on-going transmissions with which it could collide – and no more than that.

The main conclusion concerning the coexistence of DC and CSMA is that while DC has almost no effect on the CSMA system (since it can mitigate its effects by retransmitting lost packets), the opposite is not true. The significant difference in terms of performance makes CSMA a clear candidate for improving the efficiency of utilization of radio resources in SRD frequency bands. The fact that it is effectively more robust in the presence of other devices competing for the channel means that CSMA would be a much more effective choice than DC, which is specially relevant in places where a high density of sensors is expected (such as cities or homes, for instance). DC has the advantage of a higher energy efficiency, increasing the network's lifetime. In places with an expected low density of SRDs (like rural areas, where sensors could be used for environmental monitoring for agriculture), DC is the most adequate channel access scheme.

As far as the coexistence of SRDs with LTE goes, the main finding is that LTE could in fact degrade SRD performance for lower transmission powers. Increasing the power also increases the SINR, which can completely compensate for LTE's interference, from powers higher than a certain value. Nevertheless, the effects of LTE on SRDs are a theme to be considered, if the minimum performance of the latter is to be protected. On the other hand, the frequency spill of SRD's emissions onto LTE's closest channel is not significant, when compared to LTE's transmission power.

References

[1] ETSI. TS 136 101: LTE; Evolved Universal Terrestrial Radio Access (E-UTRA); User Equipment (UE) radio transmission and reception. Technical report, 2016.

[2] IMST GmbH. Channel Access Rules for SRDs. Technical report, 2012.

[3] ITU. Recommendation ITU-R P.1238-8 (07/2015). Technical report, 2015.

[4] Martocci, Jerry and Vermeylen, Wouter and Riou, Nicolas and Mil, Pieter De. Building au-

tomation routing requirements in low power and lossy networks. Technical report, IETF, 2010.

[5] I. Poole. What is noise figure. http://www.radio-electronics.com/info/rf-technology-design/rf-noise-sensitivity/noise-figure-factor.php. Accessed: 2017-04-12.

[6] C. Technology. Mica2 Datasheet. https://www.eol.ucar.edu/isf/facilities/isa/internal/CrossBow/DataSheets/mica2.pdf. Accessed: 2016-09-01.

[7] I. to Monte Carlo Methods. D. J. C. Mackay. https://www2.stat.duke.edu/courses/Spring12/sta270/lec/mcmcnotes.pdf, 2012. Accessed: 2016-09-01.